Catalysis Today 173 (2011) 21–27

Contents lists available at ScienceDirect

Catalysis Today

journal homepage: www.elsevier.com/locate/cattod

Effect of MgO activation conditions on its catalytic properties for base-catalyzed reactions

V.K. Díez, C.A. Ferretti, P.A. Torresi, C.R. Apesteguía *,[1], J.I. Di Cosimo

Catalysis Science and Engineering Research Group (GICIC), INCAPE, UNL-CONICET, Santiago del Estero 2654, 3000 Santa Fe, Argentina

ARTICLE INFO

Article history:
Received 7 December 2010
Received in revised form 20 February 2011
Accepted 28 February 2011
Available online 9 April 2011

Keywords:
MgO activation
Base-catalyzed reactions
Monoglycerides
Hydrogen transfer
Aldol condensation

ABSTRACT

The effect of the MgO calcination temperature on its basicity and catalytic properties was studied. Three MgO samples calcined at 673, 773 and 873 K (samples MgO-673, MgO-773 and MgO-873) were characterized by different physical and spectroscopic techniques. The surface base properties were probed by temperature-programmed desorption of CO_2 and infrared spectroscopy after CO_2 adsorption at 298 K and sequential evacuation at increasing temperatures. The dimensions of face-centered cubic unit cell for MgO samples decreased while crystallinity and mean crystallite size increased with calcination temperature. MgO samples contained surface sites of strong (low coordination O^{2-} anions), medium (oxygen in Mg^{2+}–O^{2-} pairs) and weak (OH^- groups) basicity. The density of strong basic sites was predominant on MgO-673, but decreased with the calcination temperature together with the density of OH^- groups; on the contrary, the density of Mg^{2+}–O^{2-} pair sites increased with calcination temperature. The catalytic properties of MgO samples were explored for the cross-aldol condensation of citral with acetone to obtain pseudoionones (PS), the transesterification of methyl oleate with glycerol to yield monoglycerides (MG), and the gas-phase hydrogen transfer reaction of mesityl oxide with 2-propanol to form 4-methyl-3-penten-2ol (UOL). The initial PS and MG formation rates decreased with calcination temperature following a trend similar to the density of strong basic sites which suggested that the rate limiting steps for both reactions involve coordinatively unsaturated O^{2-} active sites. In contrast, the initial UOL formation rate in mesityl oxide/2-propanol reaction increased with MgO calcination temperature following the same trend as medium-strength basic sites, thereby indicating that Mg^{2+}–O^{2-} pairs promote the formation of the six-atom cyclic intermediate needed in the Meerwein–Ponndorf–Verley mechanism.

1. Introduction

Lately, increasing research efforts have been devoted to the use of solid bases for obtaining fine chemicals, pharmaceuticals and valuable compounds from renewable raw materials. In particular, pure and promoted MgO has been studied for catalyzing Cannizzaro and Tischenko reactions [1], Michael, Wittig and Knoevenagel condensations [2], double-bond isomerizations [3], aldol-condensations [4], and alcohol coupling [5]. However, the MgO basicity needed for efficiently promoting these reactions depend on the rate-limiting step requirements. For example, MgO is often doped with alkali metal cations, in particular Li^+, when stronger basic active sites are needed [6]. The density, nature and strength of surface base sites on MgO depend on the preparation method. MgO is usually produced by decomposition of $Mg(OH)_2$ which in turn is obtained by different preparation methods such as sol–gel, MgO hydration, chemical vapor deposition (CVD), and precipitation. Bailly et al. [7] have reported that after $Mg(OH)_2$ decomposition at high temperature (1023 K), the relative distribution of surface low-coordination O^{2-} anions is shifted toward the less coordinated ions along the series MgO-CVD < MgO-hydration ≈ MgO-precipitation < MgO-sol–gel. The same order was observed for MgO activity to convert 2-methylbut-3-yn-2-ol into acetone and acetylene, a base-catalyzed reaction [7].

The base site properties of MgO may also be regulated by controlling both the $Mg(OH)_2$ decomposition and MgO activation conditions. For example, Vidruk et al. [8] recently reported that densification of $Mg(OH)_2$ before its dehydration to obtain MgO generates a significant increase of surface basicity. In this work, we have investigated the effect of stabilization temperature of MgO obtained by $Mg(OH)_2$ decomposition on its base and catalytic properties. Specifically, $Mg(OH)_2$ was decomposed in N_2 at 623 K and the resulting MgO was treated for 18 h in N_2 either at 673 K, 773 K or 873 K generating samples MgO-673, MgO-773 and MgO-873, respectively. The density and strength of surface base sites of MgO-*x* samples (*x* being the MgO stabilization temperature) was determined by temperature-programmed desorption of CO_2 and

* Corresponding author. Tel.: +54 342 4555279; fax: +54 342 4531068.
E-mail address: capesteg@fiq.unl.edu.ar (C.R. Apesteguía).
[1] http://www.fiq.unl.edu.ar/gicic/.

0920-5861/$ – see front matter © 2011 Elsevier B.V. All rights reserved.
doi:10.1016/j.cattod.2011.02.060

by infrared spectroscopy of CO_2 adsorbed at 298 K and desorbed at increasing temperatures. The activity and selectivity of MgO-*x* samples were probed for the liquid-phase cross-aldol condensation of citral with acetone to obtain pseudoionones (PS), the liquid-phase transesterification of methyl oleate (FAME) with glycerol to yield monoglycerides (MG), and the gas-phase hydrogen transfer reduction of mesityl oxide with 2-propanol toward 4-methyl-3-penten-2ol (UOL). Results show that the base properties of MgO, and as a consequence its catalytic properties, may be tuned by modifying the solid calcination temperature.

2. Experimental

2.1. Catalyst preparation

Three magnesium oxide samples were prepared by hydration of commercial MgO (Carlo Erba, 99%, 27 m^2/g). 250 ml of distilled water were slowly added to 25 g of commercial MgO and stirred at room temperature. The temperature was then raised to 353 K and stirring was maintained for 4 h. Excess of water was removed by drying the sample in an oven at 358 K overnight. The resulting $Mg(OH)_2$ was decomposed in N_2 (30 ml/min STP) to obtain MgO which was then treated for 18 h in N_2 either at 673, 773 or 873 K to give samples MgO-673, MgO-773 and MgO-873, respectively.

2.2. Catalyst characterization

The decomposition of $Mg(OH)_2$ was investigated by differential thermal analysis (DTA) using a Shimadzu DT30 analyzer, by temperature programmed decomposition (TPDe) using a flame ionization detector (FID) with a methanation catalyst (Ni/Kieselghur) operating at 673 K and by X-ray diffraction (XRD) in a Shimadzu XD-D1 diffractometer equipped with Cu-Kα radiation source ($\lambda = 0.1542$ nm) and a high temperature chamber. Samples characterized by X-ray diffraction were heated at 5 K/min until 773 K, taking diffractograms at 373, 573, 673 and 773 K.

Surface areas and pore volumes were measured by N_2 physisorption at 77 K using the BET method and Barret–Joyner–Halender (BJH) calculations, respectively, in an Autosorb Quantochrome 1-C sorptometer.

The structural properties of MgO-*x* samples were determined by X-ray diffraction (XRD) using the instrument described above. Analysis was carried out using a continuous scan mode at 2°/min over a 2θ range of 20–80°. Scherrer equation was used to calculate the mean crystallite size of the samples.

Sample base site densities were measured by temperature-programmed desorption (TPD) of CO_2 preadsorbed at room temperature. MgO-*x* samples were pretreated in situ in a N_2 flow at its corresponding stabilization temperature (673, 773 or 873 K), cooled to room temperature, and then exposed to a mixture of 3% CO_2/N_2 until surface saturation was achieved (10 min). Weakly adsorbed CO_2 was removed by flushing in N_2 during 1 h. Finally, the temperature was increased to 773 K at 10 K/min. Desorbed CO_2 was converted into CH_4 on a methanation catalyst and then analyzed using a FID.

The chemical nature of adsorbed surface CO_2 species was determined by infrared (IR) spectroscopy after CO_2 adsorption at 298 K and sequential evacuation at increasing temperatures. Experiments were carried out using an inverted T-shaped cell containing the sample pellet and fitted with CaF_2 windows. Data were collected in a Shimadzu FTIR Prestige-21 spectrometer. The absorbance scales were normalized to 20-mg pellets. Each sample was pretreated in vacuum at its corresponding stabilization temperature and cooled to room temperature, after which the spectrum of the pretreated catalyst was obtained. After admission of 5 kPa of CO_2 to the cell at room temperature, the samples were evacuated consecutively at 298, 373, 473, and 573 K, and the resulting spectrum was recorded at room temperature. Spectra of the adsorbed species were obtained by subtracting the catalyst spectrum.

2.3. Catalytic testing

2.3.1. Cross-aldol condensation of citral with acetone

The cross-aldol condensation of citral (Millennium Chemicals, 95% geranial + neral) with acetone (Merck, p.a.) was carried out at 353 K under autogenous pressure (≈250 kPa) in a batch Parr reactor, using acetone/citral = 49 (molar ratio) and catalyst/(citral + acetone) = 1 wt.% ratio. The reactor was assumed to be perfectly mixed and interparticle and intraparticle diffusional limitations were verified to be negligible. Reaction products were analyzed by gas chromatography in a Varian Star 3400 CX chromatograph equipped with a FID and a Carbowax Amine 30 M capillary column. Thirteen samples of the reaction mixture were extracted and analyzed during the 6-h reaction. The main product of the citral/acetone reaction was PS (cis- and trans-isomers). Moreover, diacetone alcohol and mesityl oxide were simultaneously produced from self-condensation of acetone. Trace amounts of unidentified heavy compounds were detected in the reaction mixture, probably coming from self-condensation of citral. Selectivities (S_j, mol of product *j*/mol of citral reacted) were calculated as $S_j\ (\%) = C_j \times 100/\sum C_j$, where C_j is the concentration of product *j*. Yields (η_j, mol of product *j*/mol of citral fed) were calculated as $\eta_j = S_j\, X_{Cit}$, where X_{Cit} is the citral conversion.

2.3.2. Glycerolysis of methyl oleate

The transesterification of methyl oleate, FAME (Fluka, >60.0%, with 86% total C18 + C16 esters as determined by gas chromatography) with glycerol (Aldrich, 99.0%,) was carried out at 493 K in a seven-necked cylindrical glass reactor with mechanical stirring equipped with a condenser to remove the methanol generated during reaction.

Glycerol/FAME molar ratio of 4.5 and a catalyst/FAME ratio (W_{cat}/n^0_{FAME}) of 30 g/mol were used. The reactor was operated in a semi-batch regime at atmospheric pressure under N_2 (35 cm^3/min). Liquid reactants were introduced into the reactor and flushed with nitrogen; then the reactor was heated to reaction temperature under stirring (700 rpm). Reaction products were α- and β-glyceryl monooloeates (MG), 1,2- and 1,3-glyceryl dioleates (diglycerides) and glyceryl trioleate (triglyceride). Reactant and products were analyzed by gas chromatography in a SRI 8610C gas chromatograph equipped with a flame ionization detector, on-column injector port and a HP-1 Agilent Technologies 15 m × 0.32 mm × 0.1 μm capillary column after silylation to improve compound detectability, as detailed elsewhere [9,10]. Twelve samples of the reaction mixture were extracted and analyzed during the 8-h catalytic run.

2.3.3. Hydrogen transfer reduction of mesityl oxide with 2-propanol

The gas-phase mesityl oxide/2-propanol reaction was conducted at 573 K and atmospheric pressure in a fixed bed reactor. MgO-*x* samples sieved at 0.35–0.42 mm were pretreated in N_2 at the corresponding calcinations temperature for 1 h before reaction in order to remove adsorbed H_2O and CO_2. The reactants, mesityl oxide (MO, Acros 99%, isomer mixture of mesityl oxide/isomesityl oxide = 91/9) and 2-propanol (IPA, Merck, ACS, 99.5%), were introduced together with the proper molar composition via a syringe pump and vaporized into flowing N_2 to give a N_2/IPA/MO = 93.4/6.6/1.3, kPa ratio. Reaction products were analyzed by on-line gas chromatography in a Varian Star 3400 CX chromatograph equipped with a flame ionization detector and a

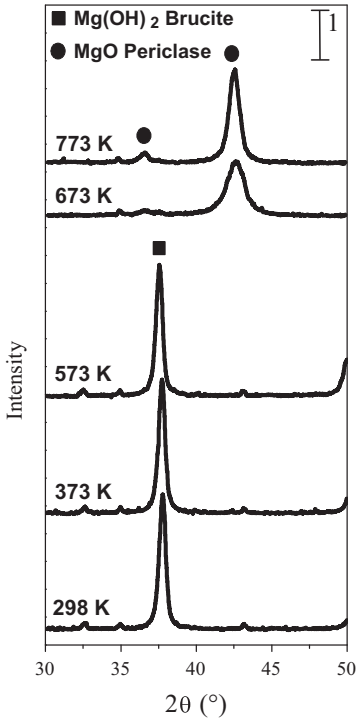

Fig. 1. XRD patterns obtained during the thermal decomposition of $Mg(OH)_2$ (high temperature chamber, 5 K/min).

0.2% Carbowax 1500/80–100 Carbopack C column. Main reaction products from mesityl oxide conversion were identified as the two unsaturated alcohol isomers (UOL, 4-methyl-3-penten-2ol and 4-methyl-4-penten-2ol), isomesityl oxide, methyl isobutyl ketone, and methyl isobutyl carbinol.

3. Results and discussion

3.1. Catalyst characterization

3.1.1. $Mg(OH)_2$ decomposition

The thermal decomposition of $Mg(OH)_2$ precursor was studied by XRD, DTA and analysis of evolved CO_2. XRD patterns in Fig. 1 shows that the $Mg(OH)_2$ brucite structure (ASTM 7-239) was stable up to about 573 K, but then, between 573 and 673 K, decomposed to MgO periclase (ASTM 4-0829) and water. Similarly, DTA results in Fig. 2 show that the $Mg(OH)_2$ heating exhibited an endothermic peak between 573 and 673 K arising from the solid decomposition; a small additional endothermic peak was observed at about 373 K, probably reflecting the loss of weakly bound adsorbed water [11]. On the other hand, TPDe experiments revealed the presence of evolved CO_2 in the 573–673 K decomposition region, thereby suggesting that the $Mg(OH)_2$ surface is reversibly carbonated by interaction with atmospheric CO_2. In summary, results of Figs. 1 and 2 show that the thermal treatment of $Mg(OH)_2$ between 575 and 675 K decomposes the solid into crystalline MgO and eliminates adsorbed carbonate species.

3.1.2. Textural and structural properties of MgO-x samples

BET surface areas of MgO-*x* samples are presented in Table 1. The MgO surface area decreased with calcination temperature, from 196 m^2/g (MgO-673) to 169 m^2/g (MgO-873). The sample pore size distribution and pore volume are presented in Fig. 3 and Table 1, respectively. It is observed that both the mean pore size and the pore volume increased with calcination temperature.

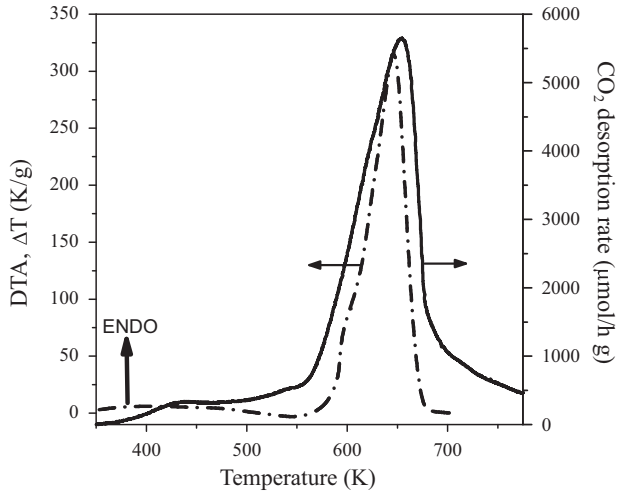

Fig. 2. Thermal decomposition of $Mg(OH)_2$ followed by DTA and evolved CO_2 (N_2 flow, 10 K/min).

The crystalline structure of MgO-*x* samples was investigated by X-ray diffraction. Diffractograms (not shown here) presented only one crystalline species of MgO periclase. The face-centered cubic unit cell dimensions for MgO-*x* samples are given in Table 1; lattice parameter (*a*) decreased with calcination temperature. Contraction of the MgO unit cell was accompanied by the increase of crystallite diameter calculated from XRD line breadths and reported in Table 1. Consistently, the sample crystallinity increased with calcination temperature from 85.4% (MgO-673) to 93.4% (MgO-873). All these results show that, as expected, the increase of the calcination temperature generated more ordered structures.

3.1.3. Surface basic properties of MgO-x samples

The surface basic properties of MgO-*x* samples were probed by TPD of CO_2 and by FTIR of CO_2 preadsorbed at room temperature and desorbed at increasing temperatures. Fig. 4 shows the IR spectra obtained for MgO-*x* samples. In previous work [12], we investigated the chemical nature of CO_2 adsorbed species on MgO by using FTIR and identified at least three different species: unidentate carbonate, bidentate carbonate and bicarbonate. Unidentate

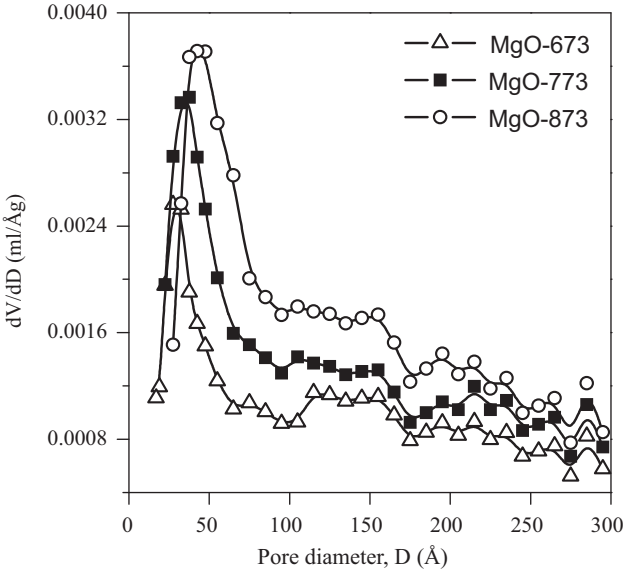

Fig. 3. Pore size distribution of MgO-*x* samples.

Table 1
Textural and structural characterization of MgO-*x* samples.

Sample	Textural characterization		XRD analysis		
	BET surface area (m^2/g)	Pore volume (ml/g)	Lattice parameter, *a* (Å)	Crystallite size (Å)	Crystallinity (%)
MgO-673	196	0.30	4.243	74.3	85.4
MgO-773	189	0.38	4.221	76.5	86.6
MgO-873	169	0.44	4.214	143.0	93.4

carbonate formation requires isolated surface O^{2-} ions, i.e. low-coordination anions, such as those present in corners or edges and exhibits a symmetric O–C–O stretching at 1360–1400 cm^{-1} and an asymmetric O–C–O stretching at 1510–1560 cm^{-1}. Bidentate carbonate forms on Lewis acid-Brønsted base pairs (Mg^{2+}–O^{2-} pair site), and shows a symmetric O–C–O stretching at 1320–1340 cm^{-1} and an asymmetric O–C–O stretching at 1610–1630 cm^{-1}. Bicarbonate species formation involves surface hydroxyl groups and shows a C–OH bending mode at 1220 cm^{-1} as well as symmetric and asymmetric O–C–O stretching bands at 1480 cm^{-1} and 1650 cm^{-1}, respectively [13–15]. The three CO_2 adsorbed species are detected on the MgO-*x* samples of Fig. 4 which present similar qualitative spectra after CO_2 evacuation at increasing temperatures. Bicarbonate was the most labile species and disappeared on all the samples after evacuation at 373 K. In contrast, both the unidentate and bidentate carbonates remained on the surface after evacuation at 473 K, but only the unidentate carbonate bands were observed upon evacuation at higher temperatures. In agreement with previous reports [12], these results suggest the following strength order for surface basic sites: low-coordination O^{2-} anions > oxygen in Mg^{2+}–O^{2-} pairs > OH groups. Fig. 4 also shows that after evacuation at or above 373 K the intensities of unidentate carbonate bands in all the samples were stronger than those of bidentate carbonate bands, thereby indicating a predominant contribution of low-coordination O^{2-} anions to the total basicity. Nevertheless, a closer inspection of the spectra of Fig. 4 reveals that the unidentate/bidentate band intensity ratio at each evacuation temperature decreased with the sample calcination temperature, i.e. from MgO-673 to MgO-873. This result may be interpreted by considering that the decomposition of $Mg(OH)_2$ at relatively low temperature, i.e. 673 K, generates hydroxylated MgO containing a high concentration of low-coordination O^{2-} sites located on defects of the crystalline solid surface. The increase of the calcination temperature removes OH groups and also surface solid defects creating a smoother and thermodynamically more stable structure, as suggested by the XRD data of Table 1.

The base site density of MgO-*x* samples was obtained by TPD of CO_2 preadsorbed at room temperature. The CO_2 desorption rate as a function of desorption temperature is presented in Fig. 5. The total base site densities of desorbed CO_2 (n_b, μmol/m^2), shown in Fig. 6 as a function of calcination temperature, were measured by integration of TPD curves of Fig. 5 and using the surface areas of Table 1. It is observed that n_b decreased with calcination temperature, from 4.58 μmol/m^2 (MgO-673) to 3.13 μmol/m^2 (MgO-873). Based on the previous IR characterization data, the TPD profiles of Fig. 5 were deconvoluted in three desorption peaks: a low temperature peak at 390 K, assigned to bicarbonates formed on surface OH groups, a middle-temperature peak at 440 K attributed to bidentate carbonates desorbed from Mg^{2+}–O^{2-} pairs, and a high-temperature peak at 550 K resulting from unidentate carbonates released from low-coordination O^{2-} anions. By integrating these three CO_2 TPD peaks we determined the density of weak (n_{OH}), medium (n_{Mg-O}), and strong (n_O) base sites, respectively. Results are presented in Fig. 6 and show that n_O and n_{OH} decreased while n_{Mg-O} increased with the MgO calcination temperature.

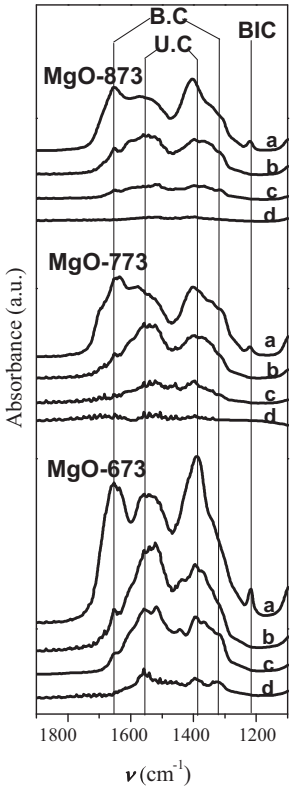

Fig. 4. IR spectra of CO_2 adsorbed on MgO-*x* catalysts at 298 K and desorbed at increasing evacuation temperatures: 298 (a), 373 (b), 473 (c), and 573 K (d) (BC: bidentate carbonate; UC: unidentate carbonate; BIC: bicarbonate).

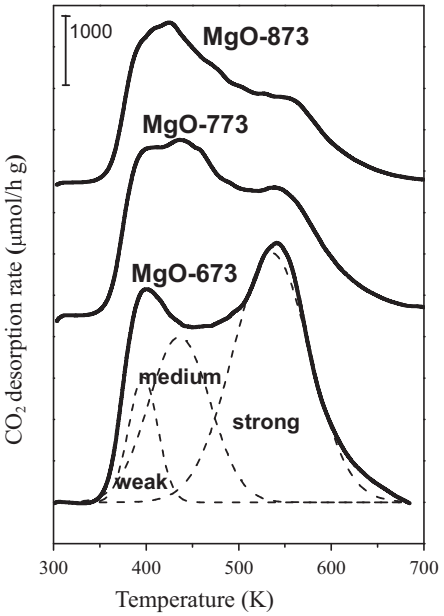

Fig. 5. CO_2 TPD profiles of MgO-*x* samples.

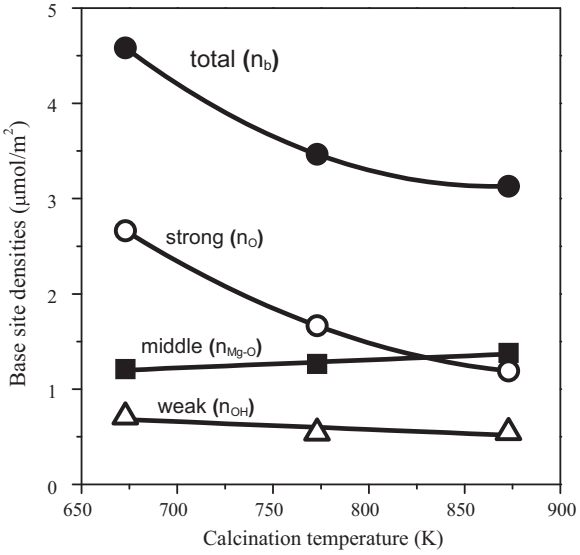

Fig. 6. Effect of MgO calcination temperature on base site densities.

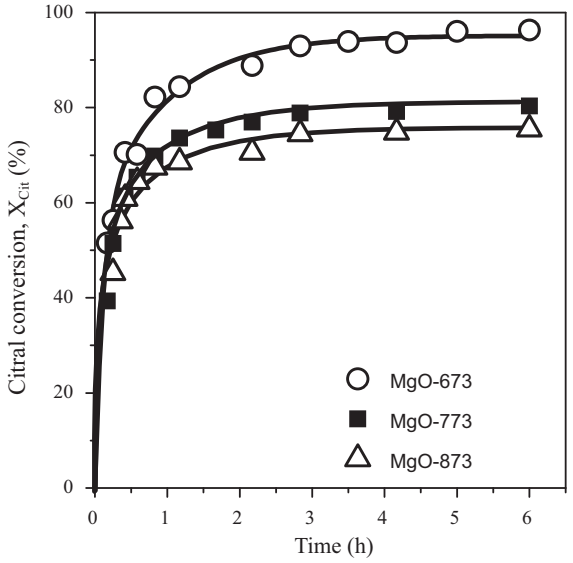

Fig. 7. Citral/acetone cross-condensation: citral conversion as a function of time (T = 353 K, n^0_{DMK} = 0.8 moles, n^0_{Cit} = 0.016 moles, W_{Cat} = 0.5 g).

3.2. Catalytic results on MgO-x catalysts

Characterization of MgO-*x* samples from data of Figs. 4–6 suggested that the MgO basicity may be regulated by modifying the calcination temperature which produces changes in density and strength distribution of surface base sites. In order to investigate the effect of MgO calcination temperature on catalyst activity, we carried out three base-catalyzed reactions on our MgO-*x* samples. Two reactions were conducted in liquid phase (cross-aldol condensation of citral with acetone, and glycerolysis of methyl oleate) and the other one in gas phase (hydrogen transfer reduction of mesityl oxide with 2-propanol).

3.2.1. Cross-aldol condensation of citral with acetone

The aldol condensation of citral with acetone produces PS (Scheme 1), a valuable acyclic intermediate for the synthesis of ionones which are extensively used as pharmaceuticals and fragrances [16,17]. This reaction has been studied using liquid [18,19] and solid [20–23] bases showing that both promote the cross-aldolization of citral with acetone simultaneously with the self-aldolization of acetone to yield diacetone alcohol and other products [23]. In particular, solid bases such as MgO and alkaline-doped MgO catalyze efficiently the selective PS formation. The reaction pathway for producing PS from the citral/acetone reaction on MgO would involve the initial abstraction of the α-proton from acetone on surface basic sites forming a carbanion intermediate that consecutively attacks the carbonyl group of the contiguously adsorbed citral molecule; Mg^{2+} cations provide the weak Lewis acid sites required to adsorb both reactants and to stabilize reaction intermediates [22,23].

The liquid-phase citral/acetone reaction was performed here on the MgO-*x* samples of Table 1. Fig. 7 shows the evolution of citral conversion (X_{Cit}) as a function of reaction time. At the end of the 6-h catalytic tests, X_{Cit} values of 96%, 80% and 75% were obtained for samples MgO-673, MgO-773 and MgO-873, respectively. On the other hand, from the curves of PS yields (η_{PS}) as a function of time (not shown here), we determined the initial PS formation rate (r^0_{PS}, mmol/h m^2) through the initial slopes according to:

$$r^0_{PS} = \frac{n^0_{Cit}}{W_{cat} S_g} \left[\frac{d\eta_{PS}}{dt}\right]_{t=0}$$

where W_{cat} is the catalyst weight and n^0_{Cit} is the molar amount of citral initially loaded in the reactor. The obtained r^0_{PS} values are plotted in Fig. 8 as a function of MgO calcination temperature. The initial PS formation rate decreased with calcination temperature, following a trend similar to the density of strong base sites in Fig. 6 (n_O values). The observed proportionality between r^0_{PS} and n_O indicates that under initial conditions the rate-determining step for PS formation is promoted by strong base sites which are predominant on sample Mg-673. In all the cases, the initial selectivities

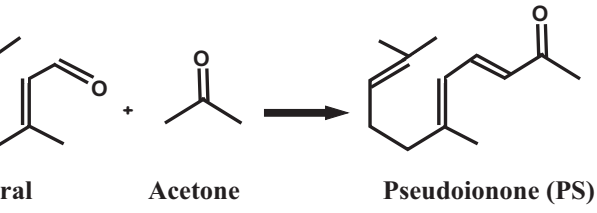

Scheme 1. Cross-aldol condensation of citral with acetone.

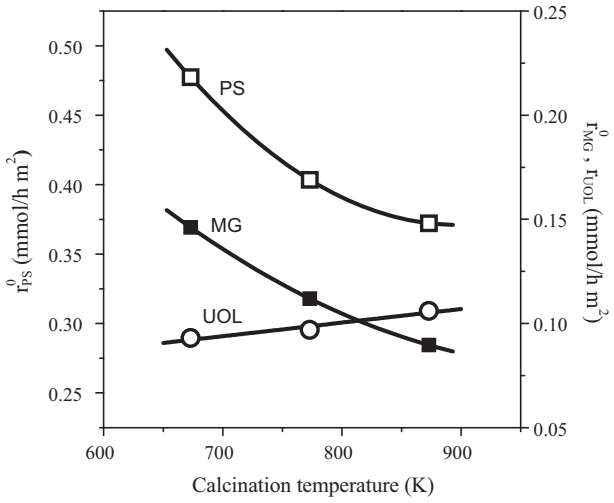

Fig. 8. Effect of MgO calcination temperature on initial formation rates of pseudoionones (reaction conditions as in Fig. 7), monoglycerides (reaction conditions as in Fig. 9), and 4-methyl-3-penten-2ol (T = 573 K, P = 101.3 kPa, N_2/IPA/MO = 93.4/6.6/1.3, W/F^0_{MO} = 15 g h/mol).

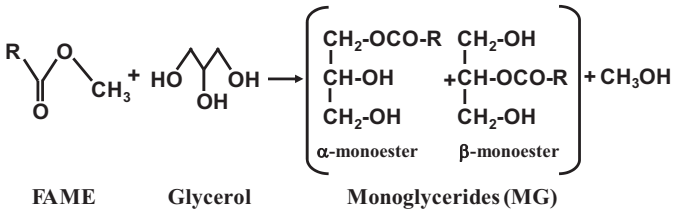

R: -$(CH_2)_7CH{=}CH(CH_2)_7CH_3$

Scheme 2. Glycerolysis of methyl oleate.

to PS were about 100%; at the end of the runs, the PS selectivities were higher than 95%, thereby showing that the conversion of citral via other reactions than its condensation with acetone is negligible.

3.2.2. Glycerolysis of methyl oleate

Biodiesel synthesis produces about 10% of glycerol as byproduct. The increasing production of low-cost glycerol due to current and future biodiesel demands causes environmental and economical concerns. Therefore, there is a need of developing novel catalytic processes to convert glycerol into valuable chemicals. In this regard, the synthesis of MG via glycerolysis of fatty acid methyl esters (Scheme 2) is an interesting option to obtain fine chemicals from bio-resources [24]. Monoglycerides are widely used as emulsifiers in food, pharmaceutical, cosmetic, and detergent industries [25]. The current technology for MG synthesis involves the use of corrosive liquid base catalysts and several neutralization and separation steps. Moreover, the homogeneously catalyzed process is not selective and forms a mixture of mono-, di-, and triglycerides. The use of solid catalysis may certainly improve this technology because they can be easily separated from the reaction media and are often reusable. MgO and MgO-based catalysts such as Mg/MCM-41 and Mg-Al mixed oxides have been investigated for the MG synthesis from glycerolysis of FAME [9,10,24,26]. Results have shown that the MG synthesis greatly depends on the nature and strength of surface basic sites as well as the catalyst pore structure.

In Fig. 9 we present the evolution of FAME conversion (X_{FAME}) with reaction time for our MgO-*x* samples. No triglycerides were formed, being 1,2- and 1,3-diglycerides the only reaction byproducts. The selectivity to monoglycerides (essentially the α-isomer) was about 75% during the entire runs. Fig. 9 shows that the MgO activity decreased with calcination temperature. For example, after 2 h of reaction the X_{FAME} values were 80%, 68% and 57% for samples MgO-673, MgO-773 and MgO-873, respectively. The initial MG formation rates (r^0_{MG}, mmol/h m^2) were determined from the curves of MG yields (η_{MG}) as a function of time (not shown here), as described above. Fig. 8 shows that r^0_{MG} decreased by increasing the calcination temperature, similarly to the density of strong base sites in Fig. 6. This result suggested that the glycerolysis of FAME to yield MG is essentially promoted on strong base sites such as the low coordination oxygen anions, in agreement with previous reports [10].

3.2.3. Hydrogen transfer reduction of mesityl oxide with 2-propanol

The selective synthesis of secondary unsaturated alcohols from reduction of alkyl vinyl ketones is an important process for pharmaceutical, fragrance and polymer industries. This reaction is not efficiently catalyzed on noble metals by conventional hydrogenation that uses high-pressure H_2 in multiphase batch reactors because of the higher reactivity of the C=C bond compared with

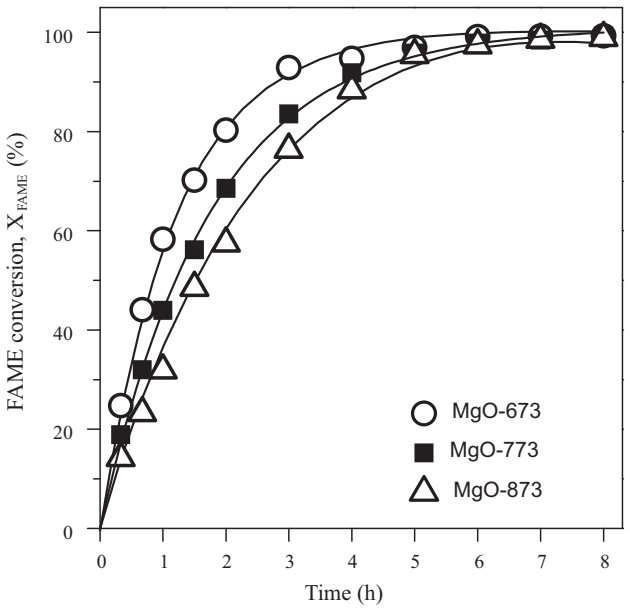

Fig. 9. Glycerolysis of FAME: FAME conversion as function of time (T = 493 K; Gly/FAME = 4.5; W_{cat}/n^0_{FAME} = 30 g/mol).

that of C=O group. Hydrogen transfer reduction (HTR) reactions may provide an alternative route for selective reduction of α,β-unsaturated ketones to the corresponding unsaturated alcohols. In the HTR reaction, the carbonyl compound (oxidant) is contacted with a hydrogen donor (reductant) at mild conditions in liquid or gas phase thereby avoiding the use of pressurized hydrogen. Heterogeneously catalyzed HTR of unsaturated carbonyl compounds would occur on metal oxides via a Meerwein–Ponndorf–Verley mechanism, which involves the selective reduction of the C=O bond preserving the C=C bond [27,28].

In particular the gas-phase HTR of mesityl oxide with 2-propanol toward the unsaturated alcohol, UOL (Scheme 3) has been studied on MgO [29,30]. UOL yields up to about 40% were obtained at 573 K using a contact time of W/F^0 = 15 g h/mol. In this work, we have employed the same operative conditions for investigating the gas-phase mesityl oxide/2-propanol reaction on MgO-*x* samples. In Fig. 8 we have plotted the UOL formation rate (r_{UOL}, mmol/h m^2) as a function of MgO calcination temperature. It is observed that r_{UOL} slightly increased with calcination temperature, similarly to the evolution of medium-strength basic sites in Fig. 6. This result suggests that the rate limiting step for the initial formation of UOL is promoted on Mg^{2+}–O^{2-} pair sites, which is consistent with previous reports [30]. In fact, as it is shown in Scheme 4 the Mg^{2+}–O^{2-} pair sites would promote formation of the six-atom cyclic intermediate needed in Meerwein–Ponndorf–Verley mechanism for preferentially transferring hydrogen from the 2-propanol donor molecule to the C=O bond of mesityl oxide. Mesityl oxide adsorbs via the C=O bond on a weak Lewis acid Mg^{2+} cation, whereas 2-propanol adsorbs non-dissociatively on a vicinal Mg^{2+}–O^{2-} pair, giving rise to the required bimolecular six-atom cyclic intermediate [29]. Then, hydride transfer occurs without participation of surface H fragments, selectively forming the unsaturated alcohol.

In summary, our results show that the density, nature and strength of surface base sites of MgO, and as a consequence its catalytic properties, change by increasing the solid calcination temperature. The effect of the calcination temperature on MgO activity and selectivity depends on the basicity requirements for the rate-limiting step of the base-catalyzed reaction.

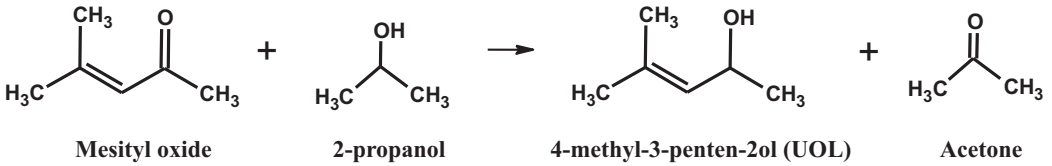

Scheme 3. Hydrogen transfer reaction of mesityl oxide with 2-propanol.

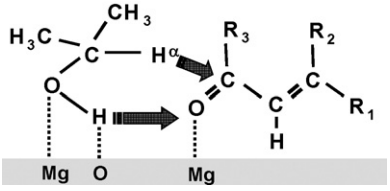

Scheme 4. Formation of reaction intermediate for HTR of mesityl oxide with 2-propanol on MgO by MPV mechanism.

4. Conclusions

Decomposition of $Mg(OH)_2$ at 623 K and stabilization of the resulting solid at 673 K generates hydroxylated MgO containing predominantly high-strength low-coordination O^{2-} basic sites located on defects of the crystalline solid surface. The increase of the calcination temperature up to 873 K removes OH groups and also surface solid defects creating a smoother and thermodynamically more stable structure containing a higher concentration of medium-strength Mg^{2+}–O^{2-} basic pair sites. Thus, the density, nature and strength of MgO surface basic sites may be regulated by modifying the solid calcination temperature.

The effect of calcination temperature on the MgO catalytic properties depends on the basicity requirements for the rate-limiting step of the base-catalyzed reaction. For example, the activity for the liquid-phase synthesis of pseudoionones by condensation of citral with acetone as well as that of monoglycerides by glycerolysis of methyl oleate diminish with MgO calcination temperature because both reactions are predominantly promoted on strongly basic O^{2-} sites. In contrast, the synthesis of 4-methyl-3-penten-2ol by the gas-phase hydrogen transfer reduction of mesityl oxide with 2-propanol is improved by increasing the MgO calcination temperature because the reaction intermediate is formed on medium-strength Mg^{2+}–O^{2-} pair basic sites.

Acknowledgements

This work was supported by the Universidad Nacional del Litoral (UNL), Consejo Nacional de Investigaciones Científicas y Técnicas (CONICET), and Agencia Nacional de Promoción Científica y Tecnológica (ANPCyT), Argentina.

References

[1] H. Tsuji, H. Hattori, Catal. Today 116 (2006) 239.
[2] A. Corma, S. Iborra, J. Primo, F. Rey, Appl. Catal. 114 (1994) 215.
[3] H. Gorzawski, W.F. Hoelderich, J. Mol. Catal. A: Chem. 144 (1999) 181.
[4] J.I. Di Cosimo, V.K. Díez, C.R. Apesteguía, Appl. Catal. 137 (1996) 149.
[5] J.I. Di Cosimo, C.R. Apesteguía, M.J.L. Ginés, E. Iglesia, J. Catal. 190 (2000) 261.
[6] V.K. Díez, C.R. Apesteguía, J.I. Di Cosimo, Catal. Today 63 (2000) 53.
[7] M.L. Bailly, C. Chizallet, G. Costentin, J.M. Krafft, H. Lauron-Pernot, M. Che, J. Catal. 235 (2005) 413.
[8] R. Vidruk, M.V. Landaua, M. Herskowitz, M. Talianker, N. Frage, V. Ezersky, N. Froumin, J. Catal. 263 (2009) 196.
[9] C.A. Ferretti, R.N. Olcese, C.R. Apesteguía, J.I. Di Cosimo, Ind. Eng. Chem. Res. 48 (2009) 10387.
[10] C.A. Ferretti, A. Soldano, C.R. Apesteguía, J.I. Di Cosimo, Chem. Eng. J. 161 (2010) 346.
[11] A. Genovese, R.A. Shanks, Polym. Degrad. Stabil. 92 (2007) 2.
[12] J.I. Di Cosimo, V.K. Díez, M. Xu, E. Iglesia, C.R. Apesteguía, J. Catal. 178 (1998) 499.
[13] C. Morterra, G. Ghiotti, F. Boccuzzi, S. Coluccia, J. Catal. 51 (1978) 299.
[14] R. Philipp, K. Fujimoto, J. Phys. Chem. 96 (1992) 9035.
[15] T. Kanno, M. Kobayashi, in: M. Misono, Y. Ono (Eds.), Acid–Base Catalysts II, Elsevier, Kodansha, 1994, p. 207.
[16] Ullman's Encyclopedia of Industrial Chemistry, Sixth edition, 2002 electronic release.
[17] E. Brenna, C. Fuganti, S. Serra, P. Kraft, Eur. J. Org. Chem. (2002) 967.
[18] P. Gradeff, US Patent 3 840 601 (1974), to Rhodia Inc.
[19] P. Mitchell, US Patent 4 874 900 (1989), to Union Camp Corporation.
[20] J.C. Roelofs, A.J. van Dillen, K.P. de Jong, Catal. Today 60 (2000) 297.
[21] M.J. Climent, A. Corma, S. Iborra, K. Epping, A. Velty, J. Catal. 225 (2004) 316.
[22] V.K. Díez, C.R. Apesteguía, J.I. Di Cosimo, J. Catal. 240 (2006) 235.
[23] V.K. Díez, J.I. Di Cosimo, C.R. Apesteguía, Appl. Catal. A: Gen. 345 (2008) 143.
[24] A. Corma, S. Hamid, S. Iborra, A. Velty, J. Catal. 234 (2005) 340.
[25] Y. Zheng, X. Chen, Y. Shen, Chem. Rev. 108 (2008) 5253.
[26] J. Barrault, S. Bancquart, Y. Pouilloux, C.R. Chim. 767 (2004) 593.
[27] G. Szollosi, M. Bartok, J. Mol. Catal. A: Chem. 148 (1999) 265.
[28] A. Corma, M.E. Domine, S. Valencia, J. Catal. 215 (2003) 294.
[29] J.I. Di Cosimo, A. Acosta, C.R. Apesteguía, J. Mol. Catal. A: Chem. 222 (2004) 87.
[30] J.I. Di Cosimo, A. Acosta, C.R. Apesteguía, J. Mol. Catal. A: Chem. 234 (2005) 111.